MPSC₆ BINUCLEAR COMPLEXES IMMOBILIZED ON GRAPHENE OXIDE FOR OXIDATION OF LIGNIN MODEL COMPOUNDS AND LIGNIN

Xue-Fei ZHOU,[a,b,c,d,e, f*] Zheng-Rong ZOU[b] and Xiao-Jun Yang[c]

[a] Chongqing Key Laboratory of Industrial Fermentation Microorganism,
Chongqing University of Science and Technology, Chongqing, 401331, China
[b] Jiangxi Provincial Key Laboratory of Protection and Utilization of Subtropical Plant Resources,
Jiangxi Normal University, Nanchang, 330027, China
[c] Key Laboratory of Green Chemical Engineering Process of Ministry of Education, School of Chemical Engineering and Pharmacy,
Wuhan Institute of Technology, Wuhan, 430205, China
[d] Key Laboratory of Exploitation and Study of Distinctive Plants in Education Department of Sichuan Province,
Sichuan University of Arts and Science, Dazhou, 635000, China
[e] Hubei Key Laboratory of Economic Forest Germplasm Improvement and Resources Comprehensive Utilization,
Hubei Collaborative Innovation Center for the Characteristic Resources Exploitation of Dabie Mountains,
Huanggang Normal University, Huanggang 438000, China.
[f] Faculty of Chemical Engineering, Kunming University of Science and Technology, Kunming, 650500, China

An efficient process for the oxidative degradation of lignin using M-GO (MPSC₆ binuclear complexes immobilized on graphene oxide) biomimetic catalysts in acetonitrile was developed in this work. Different M-GO catalysts (M=Co, Cu, Zn and Ni) were used to catalyze the depolymerization of lignin model compounds and organosolv lignin. The results showed that the immobilization of MPSC₆ complexes on GO was favorable for regulating the valuable depolymerization of the model compounds and lignin. The optimal solid catalyst Co-GO exhibited high catalytic activity, which showed a 83.04% conversion of phenolic β-O-4 lignin model compound, a 91.26% conversion of veratryl alcohol and a 96.24% conversion of vanillyl alcohol with a catalyst/model compound ratio of 50 mg:10 mmol and a dosage of 15 mmol H₂O₂ at 80 °C for 3 h. The stuctural changes of organosolv lignin occurred in catalytic oxidation were analyzed in terms of O/C ratio, molecular weight and OH content of lignin samples, and a plausible mechanism involving the formation of aromatic products and muconolactone from lignin depolymerization over M-GO was also proposed.

R₁=H, R₂=H
R₁=H, R₂=CH₃O
R₁=CH₃O, R₂=CH₃O
M-GO=MPSC₆ binuclear complexes immobilized on graphene oxide
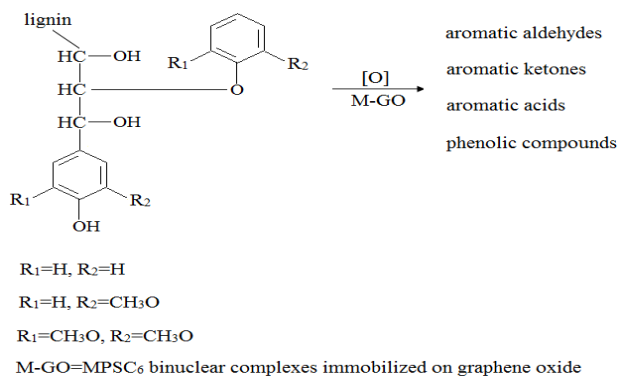
INTRODUCTION

In the papermaking industry, environmental concerns have encouraged us to develop new bleaching processes avoiding the use of chlorinated agents. Oxygen compounds have potential applications, as, for example, by the use of oxygen (O₂), hydrogen peroxide (H₂O₂), and ozone (O₃) as primary oxidants in totally chlorine-free (TCF) processes.[1] However, they unavoidably suffer from the drawbacks of poor selectivity in the pulp delignification, and ultimately leading to a low

* Corresponding author: lgdx602@sina.com

pulp yield. The lack of selectivity is due mainly to the nonselective degradation of both cellulose and lignin by oxyl radicals. One promising alternative to solve these problems is the catalytic process, where the bonds of the lignin contained in pulps are selectively cleaved, thus allowing the cellulose molecules to be retained to a greater extent.[2]

In this regard, various methods for depolymerizing lignin have been widely reported.[3] Among these, biomimetic catalysis is technologically attractive due to the chemo-enzymatic performance. Some authors have focused on depolymerization of lignin and lignin model compounds using metalloporphyrins as a catalyst.[4-6] In another research work, Zhou[7] compared the effect of Co(salen) in the catalytic treatment of Indulin lignin at 90 °C; he reported Co(salen) as being the efficient catalyst in increasing the carbonyl-compound yield and decreasing the β-O-4, β-β and β-5 linkages. In addition, several researches indicated that salen-porphyrin binuclear complexes possessed two catalytic sites within one complex, affording obvious superiority to the salen and porphyrin complexes, which led to an increasing selective conversion of substrates.[8-10] Furthermore, the previous attempts by our group of converting lignin with a salen-porphyrin complex $MPSC_6$ (Fig. 1; M=metal, P=porphyrin, S=salen, C=CH_2) have been carried out and they typically brought about high amount of vanillin, but selective transformation of lignin still need to be improved.[11] For this purpose, we promote the adhesion of the salen-porphyrin complex to the surface of graphene oxide (GO) *via* immobilization, which is based on the reported practicability as reported in literatures.[12-14]

To the best of our knowledge there is no report concerning salen-porphyrin complex-GO hybrid catalyst for lignin degradation. Therefore, the objective of the present work is to study the feasibility of a $MPSC_6$-GO catalytic process for transforming organosolv lignin (80 °C), using H_2O_2 as the oxidant and acetonitrile as the solvent. The structural changes of the lignins are described in details with elemental analysis, GPC and ^{31}P-NMR techniques. In addition, preliminary results focusing on the lignin model compounds are also presented and discussed.

EXPERIMENTAL

Materials

The following materials were commercially available and were used as received: vanillyl alcohol (Sigma-Aldrich,

96.0%), veratryl alcohol (Sigma-Aldrich, 96.0%), guaiacylglycerol-β-guaiacyl ether (GGE) (Sigma-Aldrich, 99.0%), organosolv lignin (pine sawdust, Sigma-Aldrich), *p*-hydroxyl benzaldehyde (Sigma-Aldrich, 99.0%), benzaldehyde (Sigma-Aldrich, 99.0%), salicylaldehyde, 1,6-dibromohexane (Sigma-Aldrich, 99.0%), graphite powder (325 mesh, 99.5%), potassium permanganate, concentrated sulfuric acid, cobalt (II) acetate, copper (II) acetate, zinc acetate and nickel (II) acetate. Pyrrole, *o*-phenylenediamine, 2,5-dihydroxybenzaldehyde and K_2CO_3 were purified prior to use respectively by distillation, recrystallization, column chromatography and calcination. The other materials (AR grade) were used without further treatment. Graphene oxide (GO) was prepared by oxidation of graphite powder in concentrated sulfuric acid (H_2SO_4) with potassium permanganate ($KMnO_4$) in the presence of sodium nitrate ($NaNO_3$).[15]

Milli-Q-Plus ultrapure water was used in all trials.

Preparation of catalysts

The neat binuclear complexes, $MPSC_6$ (M=Co, Cu, Zn and Ni) (Fig. 1), were synthesized as previously reported method,[11] respectively using cobalt (II) acetate, copper (II) acetate, zinc acetate and nickel (II) acetate as the metal sources. The resulting neat complexes were denoted $CoPSC_6$, $CuPSC_6$, $ZnPSC_6$, $NiPSC_6$, respectively. Spectroanalysis confirmed the successful preparation of these catalysts as follows. Elemental analysis: $CoPSC_6$: $Co_2C_{70}H_{52}N_6O_4$, 66.63% C (66.81%), 4.08% H (4.16%), 6.64% N (6.58%); $CuPSC_6$: $Cu_2C_{70}H_{52}N_6O_4$, 66.49% C (66.28%), 6.07% H (4.12%), 6.38% N (6.53%); $ZnPSC_6$: $Zn_2C_{70}H_{52}N_6O_4$, 66.28% C (66.07%), 4.21% H (4.11%), 6.73% N (6.51%); $NiPSC_6$: $Ni_2C_{70}H_{52}N_6O_4$, 66.68% C (66.84%), 4.25% H (4.16%), 6.75% N (6.58%). ^{1}H-NMR ($CDCl_3$): $(CH_2)_n$, 1.243-1.652; S-O-CH_2, 3.411; P-O-CH_2, 4.194; S-phenyl a~d, 6.972-6.976; P-phenyl 4, 7.261-7.296; S-phenyl e~k, 7.392-7.413; P-phenyl 3,5/P-phenyl 3',5', 7.772-7.877; P-phenyl 2,6/P-phenyl 2',6', 8.112-8.203; S-C=N, 8.596/8.603; p-pyrrole-H, 8.92-8.97.

The immobilized complexes were prepared as reported procedures.[16] In brief, $MPSC_6$ (0.02 g) was dissolved in N,N-dimethylformamide (DMF, 10 mL). The solution was then ultrasonically treated for 10 min and was added to a suspension of the appropriate GO (10 g) in ultrapure water (400 mL). The mixture was sonicated for 5 h at 50 °C. The resulting solid was filtered and washed with ultrapure water, and then dried at 50 °C overnight under reduced pressure. The loading capacity was ~0.6 g/mg according to the metal analysis with ICP-AES (PerkinElmer Optima 8300). The resulting immobilized complexes were denoted Co-GO, Cu-GO, Zn-GO and Ni-GO, respectively. The specific surface area was determined using the Brunauer-Emmett-Teller (BET) equation with a Micromeritics ASAP-2020 (USA). Powder X-ray diffraction (XRD) patterns of the immobilized complexes were recorded using a Rigaku Dmax X-ray diffractometer (Ni-filtered, Cu Kα radiation, 40 kV and 30 mA, 2θ, 5–40°, scanning speed 6°/min). FTIR spectra were recorded with Nicolet Impact 410 spectrometer in KBr in the scan range 400–4000 cm^{-1}. Raman spectra were obtained using a confocal micro-Raman spectrometer (Almega XR) at an excitation wavelength laser of 530 nm.

Catalytic reactions

Oxidation of lignin model compound wase undertaken in a 150 mL semi-batch reactor equipped with a stirrer. In a typical

procedure, 10 mmol of model compound, 50 ml of acetonitrile and 15 mmol of H_2O_2 were added, followed by 50 mg of catalyst (based the active species). After reaction at 80 °C for 3 h, the catalyst was filtered off and the solvent was evaporated under reduced pressure. The residues were dissolved in 25 μL of pyridine in the presence of 3,4-dimethoxytoluene as an internal standard for GC-MS analysis. For the lignin oxidation, the oxidized lignin were recovered by filtration, and the obtained lignin sample was then dried at 40 °C *in vacuum* for next analyses.

GC-MS analysis

The sample was derivatized with bis(trimethylsilyl-trifluoroacetamide) (BSTFA) prior to GC-MS analysis. The reaction products were quantified by gas chromatography-mass spectrometry (GC-MS) using a VF5-ms capillary column (30 m × 25 mm × 0.25 μm), and an isothermal temperature profile of 80 °C for the first five min, followed by a 10 °C/min temperature gradient to 280 °C, and finally an isothermal period at 280 °C for 20 min. The identification of compounds was performed by comparison with the NIST database entries or literature data and was further confirmed by the authentic compounds if available.

Elemental analysis

Elemental analysis for lignin samples was carried out with a Vario EL Elemental Analyzer 1106.

GPC

Prior to GPC analysis, lignin was treated with acetic anhydride in pyridine.[17] The molecular weight of the acetylated lignin was then determined in tetrahydrofuran with an Agilent 1100 GPC.

^{31}P-NMR

The content of various types of functional OH groups of lignin was measured with ^{31}P NMR technique on a BRUKER DRX500 NMR spectrometer using cyclohexanol as the internal standard after sample (25 mg) was phosphorized with 2-chloro-4,4,5,5-tetramethyl-1,3,2-dioxaphospholane (110 mL) in a mixture of pyridine and deuterated chloroform (0.6 mL; 1.6:1 v/v).[18]

RESULTS AND DISCUSSION

Characterization of immobilized complexes

GO, Co-GO, Cu-GO, Zn-GO and Ni-GO had BET surface areas of 616.8, 581.2, 527.1, 485.2 and 448.7 m^2/g, respectively. The low surface areas indicated the presence of Co-GO, Cu-GO, Zn-GO and Ni-GO within the supercages of the GO structure.[19]
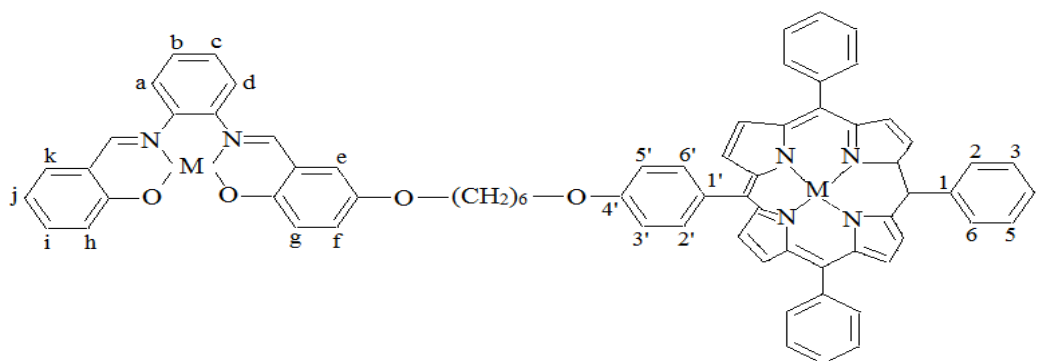
MPTPP-(CH₂)₆-salenM(MPSC₆), M=Co, Cu, Zn and Ni

Fig. 1– Structure of MPSC$_6$ complex.
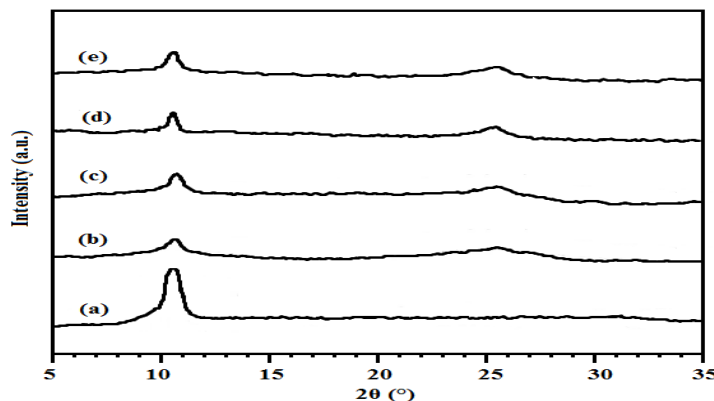
Fig. 2 – XRD spectra of (a) GO, (b) Co-GO, (c) Cu-GO, (d) Zn-GO and (e) Ni-GO.
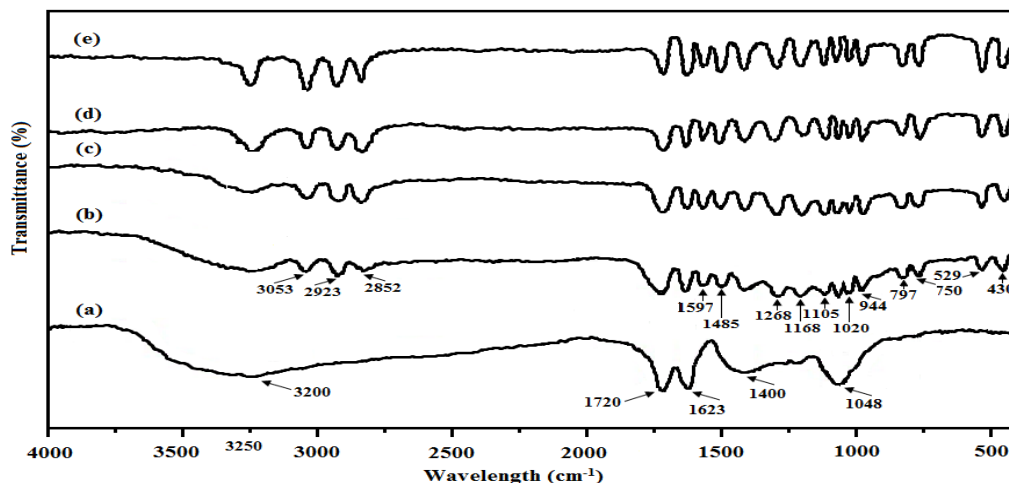
Fig. 3 – FTIR spectra of (a) GO, (b) Co-GO, (c) Cu-GO, (d) Zn-GO and (e) Ni-GO.

The obtained GO, Co-GO, Cu-GO, Zn-GO and Ni-GO samples were characterized with XRD. As shown in Fig. 2, the XRD pattern of GO displayed a diffraction peak of crystal plane at $2\theta = 10.6°$, which was due to the introduction of oxygen-containing groups, such as carboxyl, hydroxyl, epoxy between the graphite layers.[20] In addition, as shown in Fig. 2, the diffraction peaks at around 10.6° of Co-GO, Cu-GO, Zn-GO and Ni-GO samples did not disappear, indicating that the structure of GO was not destroyed after immobilization of these complexes on the GO surface. Besides, the XRD patterns of immobilized complexes (Fig. 2b,c,d,e) showed a broad peak at $2\theta = 25.5°$, confirming that the major oxygen-containing groups of GO were successfully functionalized, that is, oxygen-containing groups of GO was connected with the complex.[21]

FTIR spectra showed some groups of GO at peaks 3200 cm^{-1} (OH), 1720 cm^{-1} (C=O), 1623 cm^{-1} (C=C), 1400 cm^{-1} (C-H), 1048 cm^{-1} (C-O) (Fig. 3a), corresponding to hydroxyl, carboxyl, and epoxy groups present in GO. The Si-O-Si and Si-O-C

linkages between MPSC$_6$ (Co-GO, Cu-GO, Zn-GO, Ni-GO) and GO were also confirmed by the peaks at 1105 cm^{-1}, 1020 cm^{-1} in FTIR spectra (Fig. 3b,c,d,e).[22] In addition, the successful immobilization of MPSC$_6$ onto the GO surface was further confirmed by the bands at 3053 cm^{-1} (salenph C-H), 2923/2852 cm^{-1} (CH$_2$ C-H), 1597 cm^{-1} (salen C=N), 1485 cm^{-1} (pyrrole C=N), 1268 cm^{-1} (Ph ring C-C), 1168 cm^{-1} (Ph ring C-O), 944 cm^{-1} (Ph ring in C-H), 797/750 cm^{-1} (Ph ring out C-H), 529 cm^{-1} (M-N, M=Co, Cu, Zn, Ni), 430 cm^{-1} (M-O) (Fig. 3b,c,d,e).[11]

The catalysts were further characterized with Raman spectroscopy, and the spectra were shown in Fig. 4. The spectra indicated that the immobilization lead to broaden D bands (Fig. 4b,c,d,e). It was found that the peaks of the immobilized catalysts shifted to the G bands at 1608 cm^{-1} from the peak of GO at 1595 cm^{-1}. These changes confirmed the introduction of oxygen-containing groups, that is, the complex was connected with oxygen-containing groups of GO.[23]
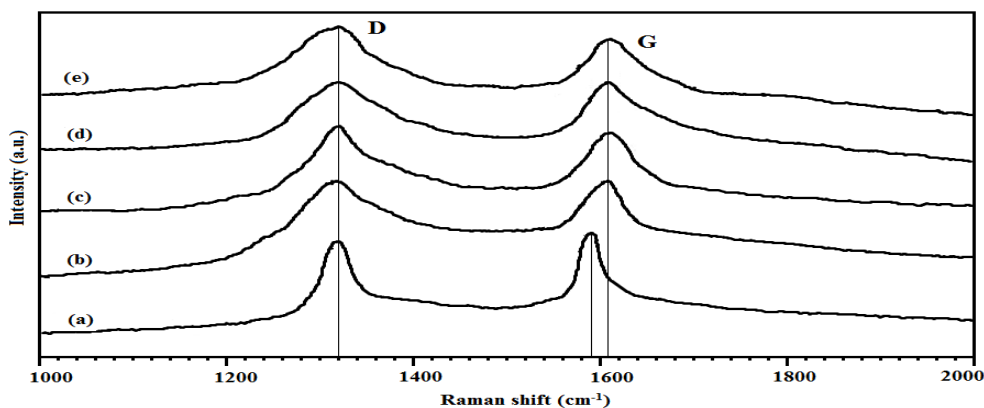
Fig. 4 – Raman spectra of (a) GO, (b) Co-GO, (c) Cu-GO, (d) Zn-GO and (e) Ni-GO.
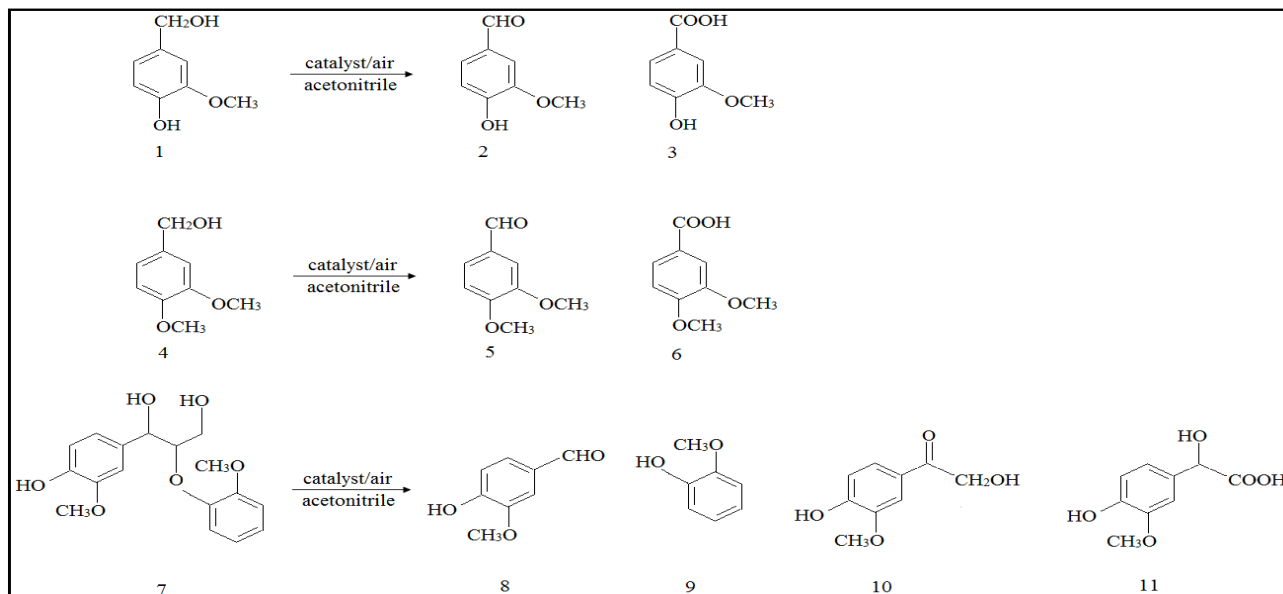
Scheme 1 – Catalytic oxidation of monomeric phenolic (1) and nonphenolic lignin model compound (4),
and dimeric phenolic β-O-4 lignin model compound (7).
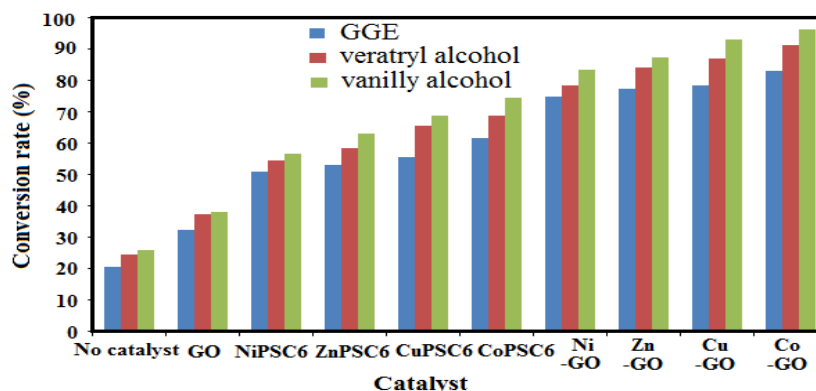
Fig. 5 – Conversion rate of vanillyl alcohol, veratryl alcohol and GGE oxidation with different catalysts.

Oxidation of lignin model compounds

It is of important interest for understanding the catalytic behavior of MPSC$_6$ complexes to elucidate the oxidation using lignin model compounds as the substrate. Consequently, three representative lignin model compounds, vanillyl alcohol (compound 1, Scheme 1), veratryl alcohol (compound 4, Scheme 1) and GGE (compound 7, Scheme 1), were studied as substrates to clarify the performance of the complexes upon phenolic and nonphenolic lignin units.

As measured using GC-MS, compared to the neat complexes, the oxidation of vanillyl alcohol by M-GO (M=Co, Cu, Zn and Ni) systems proceeded with a high conversion (Fig. 5) affording oxidation products such as vanillin (compound 2, Scheme 1) and vanillyl acid (compound 3, Scheme 1), which were most likely obtained *via* an oxidative hydrogen-

abstracting to phenolic radicals catalyzed by oxo-complex followed by alkyl side-chain oxidation.[24, 25] The efficient oxidation of vanillyl alcohol, under relatively mild reaction conditions, may be attributed to the fact that the porous structure of GO provides uniformly dispersion of active species and accessible voids for the substrate to approach the immobilized complex.[26] Furthermore, the catalysis results given in Fig. 5 showed that Co-GO displayed the expected activity in vanillyl alcohol oxidation probably because the layer structure of GO yielded more voids (see "Characterization of immobilized complexes") modifying the accessibility of the active centre,[27] which, in turn, improved the catalytic properties of the metal centre. Consequently, Co-GO presented the highest conversion of vanillyl alcohol of 96.24%, while Cu-GO gave 92.94%, Zn-GO 87.37%, and Ni-GO 83.36%.

Similarly, the oxidation of veratryl alcohol with H_2O_2 in the presence of the above catalysts gave the products of veratraldehyde (compound 5, Scheme 1) and veratric acid (compound 6, Scheme 1), which also confirmed the side-chain oxidation. However, the conversion rate of vanillyl alcohol was lower than that of veratryl alcohol (Fig. 5), which may be attributed to the more refractory non-phenolic structure.[28] Once again the highest conversion rate of 91.26% was obtained for veratryl alcohol oxidation performed with Co-GO.

In addition, it is well known that the β-O-4 dimeric compound (compound 7, Scheme 1) represents the most abundant bonding pattern in lignins.[29] Therefore, our attention was then focused on the oxidation of the compound 7 (Scheme 1). As shown in Fig. 5, the oxidation of GGE led to a appreciable decomposition of the substrate, in which a conversion rate ranged from 50.74% with $NiPSC_6$ to 83.04% of Co-GO along with cleavage at the β-position of ether bond yielding guaiacol[30] (compound 9, Scheme 1), although its conversion

rate was lower than vanillyl alcohol and veratryl alcohol. Furthermore, the indicative side-chain oxidation demonstrated a reactivity pattern close to that observed for vanillyl alcohol and veratryl alcohol, as evidenced by the presence of compound 8, compound 10 and compound 11 (Scheme 1). In a study of oxidation of β-O-4 lignin model compound with dioxygen in the presence of Co(salen) as biomimetic catalyst, Canevali *et al.*[31] also found similar behaviors.

Oxidation of organosolv lignin

Based on the clarified reactivity of M-GO catalytic systems toward lignin model compounds, attention should be payed specifically to the oxidation of the technical lignin. Therefore, these systems were employed to degrade pine organosolv lignin, and the oxidation products were detected with GC-MS, as listed in Table 1.

Table 1

Products for oxidation of organosolv lignin over $MPSC_6$ and M-GO

No.	Compound	Structure
1	Guaiacol	
2	Vanillin	
3	Phenol	
4	Vanillic acid	
5	2,6-dimethoxy phenol	
6	Syringaldehyde	

7	4-hydroxy-3-methoxyphenyl acetaldehyde
8	4-Hydroxy-3-dimethoxyphenyl ethanone
9	4-Hydroxy-3,5-dimethoxyphenyl ethanone
10	Syringic acid
11	Ferulic acid
12	4-Hydroxy-3-methoxyphenyl ethanol
13	Muconolactone
14	4-Hydroxy-3-methoxyphenyl ethyl acetate
15	4-Hydroxy-3-methoxyphenyl acetic acid

It was observed that the products of side-chain oxidation, such as aromatic aldehydes (compound 2, 6, 7; Table 1), aromatic ketones (compound 8, 9; Table 1) and aromatic acids (compound 4, 10, 11, 15; Table 1), and aromatic ester (compound 14; Table 1), were formed during catalytic oxidation of lignin; whereas the phenolic products (compound 1, 3, 5; Table 1) were simultaneously obtained. The mechanism may involve a superoxo complex (M-O-O, Scheme 2),[30,32] which abstracted phenolic hydrogen atom affording free radicals, followed by the cleaving of ether linkages and forming of double bonds at $C_1=C_\alpha$ and $C_\alpha=C_\beta$ within lignin; the former afforded phenolic products, and the latter preferentially resulted in a rapid epoxidation under the attack by the M-O-O• further giving the carbonyl compounds. Moreover, 4-hydroxy-3-methoxyphenyl ethanol (compound 12; Table 1) was most likely obtained via an addition of OH⁻ at C_β followed by formation of the methylene (-CH$_2$-) at C_α. Finally, muconolactone derivatives were likely formed by the initial oxidative ring-opening of quinone rings yielding the corresponding muconic acid derivatives followed by a stepwise oxidative degradation, probably catalysed by MPSC$_6$.[33]
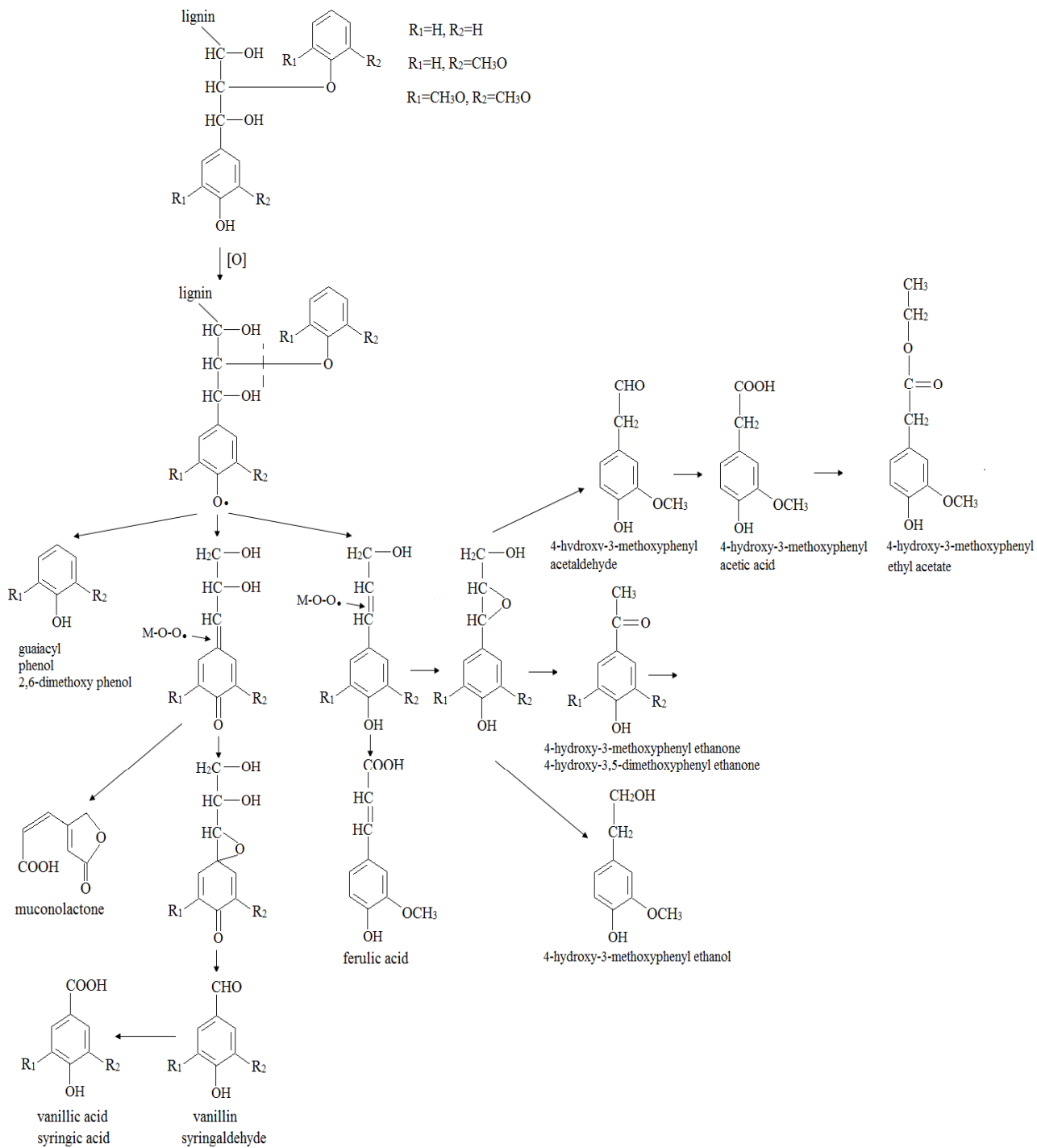
Scheme 2 – Postulated mechanism for catalytic oxidation of organosolv lignin by MPSC$_6$.

Table 2

O/C ratio, molecular weight and OH content of lignin samples

Lignin samples	O/C (n/n)	Molecular weight (M$_w$)	OH content (mmol/g)					
			Aliphatic OH	Condensed PhOH	Syringyl PhOH	Guaiacyl PhOH	*p*-PhOH	COOH PhOH
Organosolv lignin	34.53	4627	1.82	0.64	0.17	0.24	0.13	0.11
No catalyst	34.74	4603	1.80	0.63	0.18	0.26	0.14	0.13

Table 2 (continued)

GO	35.46	4568	1.76	0.62	0.21	0.28	0.15	0.14
NiPSC$_6$	37.83	3746	1.72	0.60	0.25	0.31	0.16	0.17
ZnPSC$_6$	38.37	3677	1.66	0.53	0.27	0.35	0.18	0.22
CuPSC$_6$	39.13	3621	1.65	0.52	0.29	0.37	0.23	0.27
CoPSC$_6$	40.06	3537	1.62	0.50	0.32	0.39	0.25	0.28
Ni-GO	43.73	3072	1.57	0.46	0.36	0.45	0.27	0.34
Zn-GO	44.67	2864	1.59	0.43	0.38	0.46	0.29	0.38
Cu-GO	46.33	2575	1.54	0.40	0.42	0.49	0.31	0.45
Co-GO	47.72	2257	1.51	0.28	0.46	0.53	0.35	0.47

In addition, the reaction was further elucidated according to the structural changes of organosolv lignin with catalysis by MPSC$_6$ binuclear complexes. As a whole the data indicated the oxidative degradation of lignin with enhanced catalysis, as shown in Table 2. For example, the M$_w$ sharply decreased from 4627 of organosolv lignin to 2257 of Co-GO sample, suggesting that the enhanced catalysis increasingly resulted in the fragmentation of lignin. This may be due to the degradation of linkages between lignin units such as β-O-4 substructure resulting in the formation of phenolic products observed in Table 1. The result of the progressive increase of phenolic hydroxyls (syringyl, guaiacyl and *p*-PhOH) (Table 2) further confirmed this change in the polymer. Simultaneously, an appreciable decrease in content of aliphatic OH was observed in Table 2, which was accompanied by an increase of COOH content. Meanwhile, this has been confirmed by the increasing O/C ratios. Particularly and importantly for deep degradation of lignin, when compared with the other catalysts in Table 2, Co-GO afforded an extensive decrease in content of condensed PhOH that is refractory lignin units. These findings are consistent with the obtained results from the analysis aboult the oxidation products that the catalytic reactivity of MPSC$_6$ complexes could be increased by immobilization on graphene oxide. Thus, it may be proposed that Co-GO possessed a superiority in lignin degradation over other neat and immobilized MPSC$_6$ complexes.

CONCLUSIONS

This study suggests that M-GO (MPSC$_6$ immobilized on graphene oxide, M=Co, Cu, Zn and Ni) catalyst was much effective in degrading lignin model compounds and organosolv lignin. This was the result of the two catalytic sites within one complex, porous structure of GO, and well-dispersion of active species in GO. Co-GO, never used before in lignin degradation, showed to be the best catalyst among these tested catalysts in oxidation of both phenolic and nonphenolic lignin model compounds, so that the organosolv lignin was decomposed to the greatest extent, affording the most structural modifications, especially the condensed substructures, in the Co-GO catalyzed oxidation.

REFERENCES

1. F. Beltramino, M. B. Roncero, T. Vidal and C. Valls, *Afinidad*, **2018**, *75*, 91–96.
2. G. Afsahi, E. I. Ferro, K. Ruuttunen and T. Vuorinen, *J. Wood Chem. Technol.*, **2019**, *39*, 178–186.
3. Y. H. Chan, K. W. Cheah, B. S. How, A. C. M. Loy, M. Shahbaz, H. K. G. Singh, N. R. Yusuf, A. F. A.

Shuhaili, S. Yusup, W. A. W. A. Ghani, J. Rambli, Y. Kansha, H. L. Lam, B. H. Hong and S. L. Ngan, *Sci. Total Environ.,* **2019**, *680*, 105–123.

4. L. Yan, C. Jie and O. Yong, *Adv. Mater. Res.,* **2013**, *805–806*, 273–276.

5. C. Zhu, W. Ding, T. Shen, C. Tang, C. Sun, S. Xu, Y. Chen, J. Wu and H. Ying, *Chem. Sus. Chem.*, **2015**, *8*, 1768–1778.

6. S. L. Bharati, C. Sarma, P. J. Hazarika, K. Chaurasia, N. Anand and S. Yadava, *Russ. J. Inorg. Chem.,* **2019**, *64*, 335–341.

7. X.-F. Zhou, *Bulgarian Chem. Comm.,* **2018**, *50*, 615–620.

8. K. Maruyaama, F. Kobayashi and A. Osuka, *Bull. Chem. Soc. Jpn.,* **1990**, *63*, 2672–2681.

9. X.-J. Zhao, W.-J. Ruan and Z.-A. Zhu, *Chinese J. Org. Chem.,* **2006**, *26*, 1087–1092.

10. P. Ju, S. Wu, Q. Su, X. Li, Z. Liu, G. Li and Q. Wu, *J. Mater. Chem. A,* **2019**, *7*, 2660–2666.

11. X.-J. Lu, X.-F. Zhou, Z.-L. Zhu, Y. L. Sun, K. Tang, F.-H. Lei, Z.-G. Liu and T. Wang, *Drewno,* **2019**, *62*, 67–80.

12. S. Yu, L. Chen and Z. Yan, *Bioresources,* **2017**, *12*, 2354–2366.

13. X.-F. Zhou and X.-J. Lu, *J. Appl. Polym. Sci.,* **2016**, *133*. DOI:10.1002/app.44133.

14. Z. Yuan, S. Chen and B. Liu, *J. Mater. Sci.,* **2017**, *52*, 164–172.

15. W. S. Jr. Hummers and R. E. Offeman, *J. Am. Chem. Soc.,* **1958**, *80* 1339.

16. P. R. Cooke and J. R. L. Smith, *J. Chem.Soc. Perk. Trans.,* **1994**, *1*, 1913–1923.

17. J. M. Macleod, *Paperi ja Puu,* **1990**, *72*, 780–787.

18. F. Araya, E. Troncoso, R. T. Mendonca and J. Freer, *Biotechnol. Bioeng.,* **2015**, *112*, 1783–1791.

19. I. Ali and T. A. Saleh, *Appl. Catal. A-Gen.,* **2020**, *598*. DOI: 10.1016/j.apcata.2020.117542.

20. S. M. Anush, H. R. Chandan, B. H. Gayathri, Asma, N. Manju, B. Vishalakshi and B. Kalluraya, *Int. J. Biol. Macromol.,* **2020**, *164*, 4391–4402.

21. S. M. G. Yek, D. Azarifar, M. Nasrollahzadeh, M. Bagherzadeh and M. Shokouhimehr, *Sep. Purif. Technol.,* **2020**, *247*. DOI: 10.1016/j.seppur.2020.116952.

22. I. Parra, S. Valbuena and F. Racedo, *Spectrochim. Acta. Part A,* **2021**, *244*, 118833. DOI:10.1016/j.saa.2020.118833.

23. N. Duan, M. F. Shen, S. J. Wu, C. X. Zhao, X. Y. Ma and Z. P. Wang, *Microchim. Acta,* **2017**, *184*, 2653–2660.

24. Y. M. Sun, J. S. Wu and C. B. Liu, *Chinese Sci. Bull.,* **2007**, *52*, 1182–1186.

25. B. Rahmanivahid, M. Pinilla-de Dios, M. Haghighi and R. Luque, *Molecules,* **2019**, *24*, DOI:10.3390/molecules24142597.

26. P. R. G. N. Reddy, B. G. Rao, T. V. Rao and B. M. Reddy, *Catal. Lett.,* **2019**, *149*, 533–543.

27. H. Su, S. Wu, Z. Li, Q. Huo, J. Guan and Q. Kan, *Appl. Organometal. Chem.,* **2015**, *29*, 462–467.

28. X. Qin, X. Sun, H. Huang, Y. Bai, Y. Wang, H. Luo, B. Yao, X. Zhang and X. Su, *Biotechnol. Biofuels,* **2017**, *10*. DOI:10.1186/s13068–017–0787–z.

29. R. A. Maia, G. Ventorim and A. B. Neto, *J. Mol. Model.,* **2019**, *25*. DOI:10.1007/s00894–019–4130–4.

30. H. R. Wu, J. L. Song, C. Xie, C. Y. Wu, C. J. Chen and B. X. Han, *ACS Sust. Chem. Eng.,* **2018**, *6*, 2872–2877.

31. C. Canevali, M. Orlandi, L. Pardi, B. Rindone, R. Scotti, J. Sipilä and F. Morazzoni, *J. Chem. Soc. Dalton, Trans.,* **2002**, *15*, 3007–3014.

32. Y. Shimazaki and O. Yamauchi, *Indian J. Chem.,* **2011**, *50A*, 383–394.

33. Z. Wu, J. Zhang, Q. Pan, X. Li, Y. Zhanga and F. Wang, *RSC Adv.,* **2018**, *8*, 12344–12353.